A highly sensitive frontend IC for very robust capacitive vortex flowmeter sensors

Hanspeter Schmid*, Alex Huber*, Dirk Sütterlin‡, Werner Tanner‡
*University of Applied Sciences Northwestern Switzerland (FHNW), Institute of Microelectronics (IME)
‡Endress+Hauser Flowtec AG
{hanspeter.schmid, alex.huber}@fhnw.ch {Dirk.Suetterlin, Werner.Tanner}@flowtec.endress.com

***Abstract*—This paper presents a capacitive sensor interface IC for vortex flow measurements. With this interface, we can measure flows down to half the minumum flow speed of the state of the art, for media temperatures up to $400\,^{\circ}\mathrm{C}$ and pressures up to 200 bar in pipes from 15 mm up to 300 mm diameter, even in the presence of mechanical vibrations, for media ranging from air over oil to mercury. The mechanical sensor used is very robust in the presence of steam hammers.**

The sensor IC was realized in $0.35\,\mu\mathrm{m}$ CMOS and operates over a temperature range of $-50\ldots125\,^{\circ}\mathrm{C}$. It adds input-referred noise far below the $\mathrm{kT/C}$ noise of the sensor, $1.17\,\mathrm{aF}/\sqrt{\mathrm{Hz}}$ at $\mathrm{f_s} = 128\,\mathrm{kHz}$. The IC consumes $1.5\,\mathrm{mA}$ from a $3.3\,\mathrm{V}$ supply and has an area of $10\,\mathrm{mm}^2$. The main signal processing problems to solve were the compensation of time-varying offsets up to 8 pF while measuring 60 aF, and the digital detection of signal frequencies at $1.15\,\mathrm{dB}$ SNR, done by adaptive filtering. The sensor IC has a production yield of $96.5\,\%$.

I. Introduction

There are many measurement principles known so far for measuring fluid flow. The most precise one, the Coriolis principle, is not robust in the presence of steam hammers. If a steam hammer of sufficient strength occurs, the whole precision-mechanical sensor element suffers total damage.

The vortex measurement principle shown in Fig. 1 uses a much smaller sensor that is more robust to steam hammers. Both the precision and the price of vortex flowmeters are a decade below those of Coriolis flowmeters. Coriolis flowmeters are, however, used in the production calibration of vortex flowmeters.

The vortex principle works as follows: an obstacle, called *bluff body*, is inserted into the tube. As soon as the flow becomes turbulent, which approximately is the case when the Reynolds number becomes larger than 4000, the medium starts shedding vortices at the bluff body, alternatively one to the left and one to the right. The medium's volume per vortex is constant, and the vortex shedding frequency $f_v = Q/k_{\mathrm{cal}}$, where Q is the volume flow in m^3/s and k_{cal} depends on the inner dimensions of the pipe and on the bluff body geometry. The vortex shedding frequency can then be measured by using a mechanical sensor (paddle) as we do, by using pressure sensors, piezo sensors, or even microphones.

Such a measurement device needs to cover a huge signal magnitude range. For one medium in one pipe, the amplitude of the vortex oscillation is proportional to the square of the flow velocity. The targeted turn-down of a flow meter is 1:100, meaning $1\,\%$ of the maximum flow can still be measured accurately. This translates to an amplitude range of 1:10000. The amplitude also depends on the density ρ of the medium. Since the same sensor element can be used in pipes ranging from DN 15 (15 mm diameter) to DN 300, and be used to measure media ranging from air over water and oils to mercury, the range of signal magnitudes to be covered is $102.5\,\mathrm{dB}$, from $60\,\mathrm{aF}$ to $8\,\mathrm{pF}$.

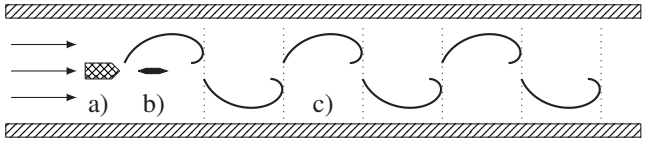

Figure 1: Vortex counting principle shown in the horizontal cross section of a pipe. a) bluff body extending vertically through the whole pipe; b) short sensor paddle sticking into the fluid flow; c) Kármán vortex street. A 3D animation of the sensor operation can be found on [1].

In addition to this, the sensor needs to operate at temperatures between $-200\ldots400\,^{\circ}\mathrm{C}$, so it is impossible to place the sensor interface IC close to the sensor. The sensor needs to operate up to PN 250 (250 bar pressure in the pipe), so its membrane is very stiff. We are therefore facing a situation where a capacitive sensor gives a maximum capacitive difference signal of $6.8\,\mathrm{pF}$ and a minimum signal of $60\,\mathrm{aF}$, but has large and time-varying parasitic capacitances because of the long cable between sensor and IC and thermically isolating connectors.

The main technical problem to solve is to build a high-resolution offset-compensation scheme that does not compromise noise performance. In addition, the signal magnitudes for very low flows become so small that simple vortex counting is not possible anymore, so we also introduce an adaptive-filter-based detection system for low signals.

The state of the art for vortex flowmeters in the market is that the minimum flow velocity which can be measured is $v = \frac{6}{\sqrt{\rho}}\,\frac{\mathrm{m}}{\mathrm{s}}$ for DN 15 to DN 25 and $\frac{7}{\sqrt{\rho}}\,\frac{\mathrm{m}}{\mathrm{s}}$ for DN 40 to DN 300, where ρ is the density of the medium in $\mathrm{kg/m}^3$ and the reference quantity in the numerator has the unit $\sqrt{\mathrm{kg/m}^3}$. One example is the Prowirl by Endress+Hauser [1]. Vortex flowmeters without moving mechanical parts (different sensor design) and similar temperature ranges, like the Foxboro 83F, go down to $v = \frac{4.8}{\sqrt{\rho}}\,\frac{\mathrm{m}}{\mathrm{s}}$, but only cover pressures up to $100\,\mathrm{bar}$.

In this paper, we present the relevant electronics and signal-processing scheme that make it possible to reach a minimum flow velocity of $\frac{3.5}{\sqrt{\rho}}\,\frac{\mathrm{m}}{\mathrm{s}}$ in DN 15 to DN 300 with a capacitve-based mechanical sensor. Because the amplitude is proportional to the square of the flow velocity, we have effectively improved the state-of-the-art SNR by $(7/3.5)^2 = 12\,\mathrm{dB}$.

II. Operating Principle and Offset Compensation

Figure 2 shows a simplified block diagram of the measurement path. The sensor element is a paddle behind a bluff body,

978-1-4799-5696-8/14/$31.00 ©2014 IEEE

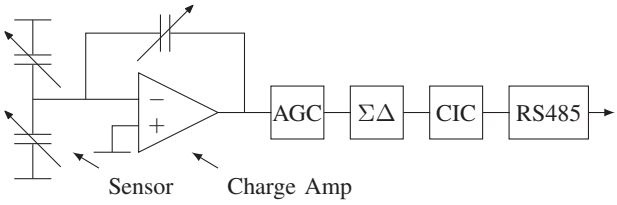

Figure 2: Simplified block diagram of the sensor IC.

set in a very stiff membrane. A capacitive element on the other side of the membrane translates paddle movements to capacitance differences δC. The maximum δC caused by a vortex signal is $\pm 6.8\,\mathrm{pF}$. This δC is measured with a charge amplifier, amplified by a switched-capacitor automatic-gain-control amplifier (AGC), and then converted by a second-order $\Sigma\Delta$ modulator.

The sensor amplifier is a charge amplifier working with correlated double sampling (CDS). The total gain of this amplifier together with the AGC is adjustable from $0.18 \ldots 24\,\mathrm{V/pF}$. It measures dynamic capacitance differences between the sensor capacitors up to $8\,\mathrm{pF}$, where the sum of all sensor and parasitic capacitors can be up to $200\,\mathrm{pF}$.

The high gains required for this measurements can saturate the amplifiers and the $\Sigma\Delta$ modulator in the presence of offset capacitances; the system must be able to compensate these offsets. The range of compensation is $\pm 12\,\mathrm{pF}$ with a resolution of $15.625\,\mathrm{fF}$, with 9 bits in a binary code and a tenth bit that has the same weight as the 9^{th} bit. Note that the sole purpose of gain adjustment and offset compensation is to not saturate the ADC. So both can be done simply by observing the ADC output. The system is then effectively AC coupled, which is no problem as we want to measure an oscilation frequency.

The offset compensation works as follows: In a first phase of this compensation, a capacitance of the C-array (Fig. 3) is pre-charged to V_{refp} or V_{refn}, depending on the direction of the compensation. In the next phase, the capacitance is discharged into the charge amplifier. The value of the capacitance needed to compensate for offset is set by digitally controlled switches.

Since the parasitic capacitances of the switches are large compared to the step size of $15.625\,\mathrm{fF}$, dummy switches are used to compensate the parasitics. This compensation works as follows: In the first phase, when the C-array is charged to V_{refp} (V_{refn}), the dummy switches are connected to opposite voltage V_{refn} (V_{refp}). Hence, the charges stored in the C-array path and the dummy path are $Q_{\mathrm{Coff}} + Q_{\mathrm{Cp,sw}}$ and $-Q_{\mathrm{Cp,sw}}$, respectively. Discharging both paths to the charge amplifier, the charges are added, so only Q_{Coff} is transferred to the charge amplifier.

However, the absolute values of the charges stored on the switches are not exactly equal when connecting them to V_{refp} and V_{refn}. Hence this compensation only works properly when two additional phases are used to charge the C-array and the dummy switches to the opposite voltages they had in the first phase, and then again discharge them into the charge amplifier. This is done synchronously to the two phases needed for correlated double sampling in the signal path.

To simulate the behaviour of the offset compensation, an offset δC is applied to the sensor capacitance which has the same value as the programmed C_{off}. The error of the output of charge amplifier is then determined. From this error,

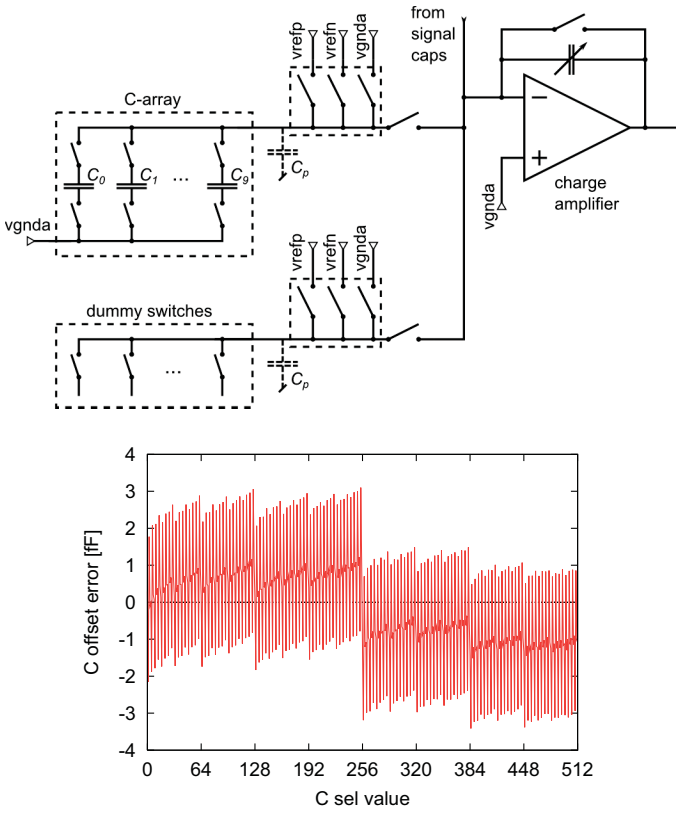

Figure 3: Offset compensation circuit and simulated performance.

the difference to an ideal offset compensation is calculated. The results are shown in Fig. 3 for offset capacitances from $0 \ldots 7.98\,\mathrm{pF}$, which are the lower nine of the ten bits. In this range, the error remains within $\pm 3.5\,\mathrm{fF}$.

The switch matrix, charge amplifier, and SC amplifier typically consume $17\,\mu\mathrm{A}$, $310\,\mu\mathrm{A}$, and $175\,\mu\mathrm{A}$ from the $3.3\,\mathrm{V}$ supply.

III. Sigma-Delta Modulation and CIC Filter

This offset-compensated, gain-controlled signal is then converted to a digital data stream. The vortex frequency range to be detected covers $0.1 \ldots 4000\,\mathrm{Hz}$ over the whole range of pipe diameters and media. Since the magnitude of vortex signals is proportional to the square of the frequency, the natural choice is a simple second-order $\Sigma\Delta$ modulator, whose noise transfer function shows the same frequency behaviour. The sampling frequency of both the $\Sigma\Delta$ modulator and the whole measurement path in front of it is $f_s = 128\,\mathrm{kHz}$, and the DC signal gain of the $\Sigma\Delta$ modulator is $1/(1.5\,\mathrm{V})$.

The goal is to measure the frequency, not the magnitude, so f_s must be precise and stable. It is generated by an on-chip low-power $10.24\,\mathrm{MHz}$ crystal oscillator.

The analog part of the $\Sigma\Delta$ modulator, its digital part, and the oscillator typically consume $70\,\mu\mathrm{A}$, $40\,\mu\mathrm{A}$, and $58\,\mu\mathrm{A}$ from the $3.3\,\mathrm{V}$ supply.

In the standard configuration, the $\Sigma\Delta$ bitstream is sent to a remote transmitter unit (containing a microprocessor, a low-power signal processor and a 4–20-mA interface) using a low-power RS485 interface. In the extreme case, that unit can

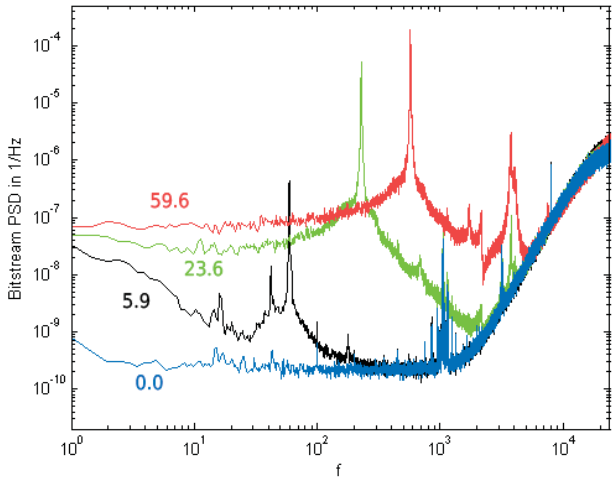

Figure 4: Bitstream spectra from measurements made with air under a pressure of 2 bar. Bottom upwards: 0 l/s, 5.9 l/s, 23.6 l/s, 59.6 l/s.

be 30 m away from the PCB containing the sensor interface. Therefore the IC also contains a configurable CIC (cascaded integrator comb) filter that can down-sample the bitstream to a wide range of intermediate frequencies and truncate the CIC output bit width, and therefore reduce the required bandwidth and power on the RS485 line. A copy of the same $\Sigma\Delta$+CIC block is also used for the single-shot conversions described in Sec. VI.

IV. Analog Measurement Results

Measurements were made with several test systems and a real sensor in a pipe, as shown in Fig. 5. This setup can produce a fully developed turbulent flow profile on air. The medium used for this measurement was air at 2 bar pressure; and a 50 mm pipe (DN50) was used. Measurements at high pressures and temperatures look very similar. The $\Sigma\Delta$ bitstream was recorded for different flow speeds.

Fig. 4 shows the power spectral densities of bitstreams measured for different flows. The lowest curve is zero flow and shows the noise behaviour of the system, including some electrical interference from the RS 485 communication around 1 kHz into the sensor connector on the PCB. The spectrum of the lowest detectable signal looks just like the lowest curve; for the measurement time and averaging used here, no peak is visible.

The quadratic dependence of the magnitude compared to the frequency is well visible between the second and third curve from the bottom. The fourth curve shows considerably less magnitude than the reader might expect, because in this situation the automatic gain control of the system has changed the gain setting to prevent ADC overload. A significant increase of low-frequency noise is visible for increasing flow. This is, however, not electronic noise, but acoustic noise caused by the turbulent flow in the pipe (i.e., the "whoosh" sound you hear when you hold your ear next to the pipe). The increase towards high frequencies is the $\Sigma\Delta$ quantization noise.

The maximum gain used in this measurement was $G = 24\,\mathrm{V/pF}$, which translates to a gain from the differential capacitance to the digital bitstream of $G = 16/\mathrm{pF}$. The noise floor of the lowest curve, $3.5049 \cdot 10^{-10}/\mathrm{Hz}$, corresponds to an input-referred noise of $1.17\,\mathrm{aF}/\sqrt{\mathrm{Hz}}$. This is the kT/C noise of the sensor together with all parasitic capacitances sampled at 128 kHz.

These (and other) measurements show that the offset compensation works, and that the IC, with all parasitic effects, substrate noise, etc., adds much less input-referred noise than $1.17\,\mathrm{aF}/\sqrt{\mathrm{Hz}}$ to the noise floor. The $1/f$ noise corner frequency could not be measured precisely; it is below 2.5 Hz.

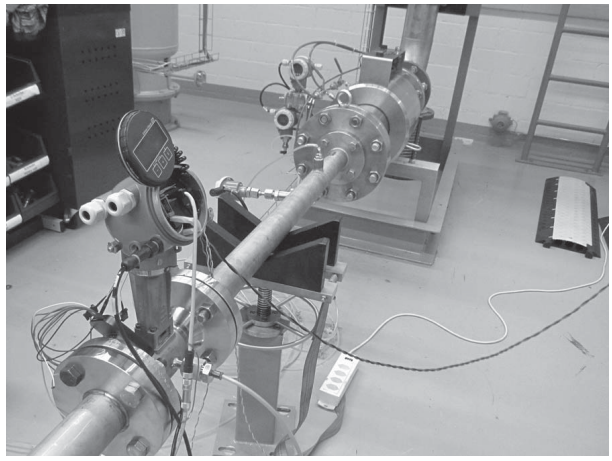

Figure 5: Measurement setup.

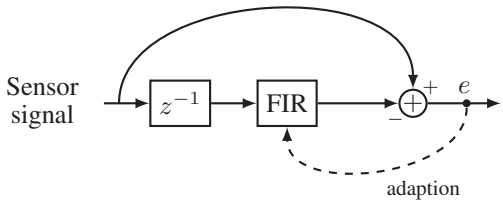

Figure 6: Signal spectrum identification by linear predictive estimation with an adaptive filter of, e.g., length $N = 11$. When the filter adapts, the FIR zeros go to the signal poles.

V. Frequency Detection

The vortex shedding frequency can be measured simply by counting zero transitions in the signal if the signal is large enough. Towards very low signal magnitudes, noise makes this impossible. For the lowest signal, 60 aF, and a signal bandwidth of 1 kHz, the SNR is 1.15 dB. In addition, the vortex street is a mildly non-linear chaotic oscillator whose output spectrum resembles that of a second-order low-pass filter with a pole frequency f_p, a resonance frequency $f_0 < f_p$ (which is the average vortex shedding frequency), and a medium-range pole quality factor, e.g., $q_p = 100$. Prominent mechanical sinusoidal vibrations on the pipes have $q_p \gg 100$. Estimating the q_p together with the f_0 therefore makes it possible to distinguish between a vortex shedding signal and mechanical vibrations.

One way to estimate f_0 is to use an adaptive FIR filter as a linear predictive estimator and search the peaks in the inverse of the magnitude plot of the FIR filter [2], [3]. This can be done because the zeros of the FIR filter will move to the poles of the spectrum of the measured signal; the FIR

filter then works as a system identifier. A block diagram of this estimator is shown in Fig. 6.

The new method we use [4] does not estimate the magnitude, but directly calculates f_0 and q_p from the FIR coefficients. The FIR filter zeros are in the z-domain, whereas the vortex street is a continuous-time system that has poles in the s domain. Using the impulse-invariant transform, we can calculate which z-domain zeros z_p a complex s-domain pole pair with pole frequency ω_p, resonance frequency ω_0, and pole quality factor q_p will cause. Then, given a complex zero of the FIR filter, we calculate

$$z_r = \mathrm{Re}\{z_p\}, \quad z_i = \mathrm{Im}\{z_p\}, \quad z_a = \sqrt{z_r^2 + z_i^2}; \quad (1)$$

$$\Sigma = \ln z_a, \quad \Omega = \pm \cos^{-1}\left(\frac{z_r}{z_a}\right), \quad (2)$$

$$\sigma_p = \frac{\Sigma}{T_s}, \quad \omega_0 = \frac{\Omega}{T_s}, \quad (3)$$

$$\omega_p = 2\pi f_p = \sqrt{\omega_0^2 + \sigma_p^2}, \quad q_p = -\frac{\omega_p}{2\sigma_p}. \quad (4)$$

This is implemented on a fixed-point-arithmetic low-power DSP. The FIR filter uses a low-power-optimized version of the ERLS algorithm [5] for adaptive filtering and a low-power fixed-point implementation for finding the zeros of the filter polynomial. Since the adaptive filter already applies smoothing, the zeros only need to be calculated, e.g., once per millisecond. Extensive experiments made with air, steam and water flows have shown that this method can measure very low flow frequencies to within a precision of $\pm 0.1\,\%$ for different media, and extends the measurement limit down to $\frac{3.5}{\sqrt{\rho}}\,\frac{\mathrm{m}}{\mathrm{s}}$ as expected. The method can also distinguish vortex signals from vibrations. (The reference measurements to compare our method against were made by using a very-narrow-band filter manually set to the approximate vortex shedding frequency followed by a zero-crossing counter.)

VI. System performance summary

In addition to the vortex signal, the sensor interface IC can also measure the temperature of the sensor by measuring a PT1000 resistor in the sensor element and doing single-shot $\Sigma\Delta$ conversion. The sum of the sensor capacitances can be measured likewise, as well as the leakage current in the sensor capacitors. Those two values indicate whether a steam hammer has bent the paddle element (total capacitance) or cracked the sensor membrane (leakage) beyond usefulness.

The measurements and offset compensation can only be done with the required precision if the two voltages V_{refp} and V_{refn} mentioned above are symmetric to analog ground. A precise symmetry is forced by trimming a reference resistor array during the IC production test, and storing the trimming values in an on-chip ROM. This requires voltage trimming to within $\pm 300\,\mu\mathrm{V}$, which takes an average time of $1.5\,\mathrm{s}$ during package-level production test.

The chip has been designed and laid out in a $0.35\,\mu\mathrm{m}$ low-leakage CMOS process. The photo of one chip corner is shown in Fig. 7. It is already in mass production. Measurements made during the production test for all 5480 samples of two fabricated wafers show a total current consumption of $0.63 \ldots 0.72\,\mathrm{mA}$ in the analog part and $0.76 \ldots 0.82\,\mathrm{mA}$ in the digital part, in a mode where the IC continuously measures the sensor signal and communicates over a short RS485 line. The production yield was $96.5\,\%$.

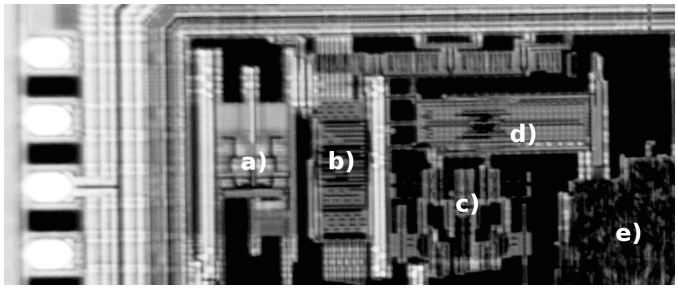

Figure 7: Chip photo: a) analog buffers for test outputs, b) offset-compensation array, c) charge amplifier with d) gain-control capacitor, e) corner of the digital controller.

A recently published, similar capacitive sensor front-end targeted at a $1 \ldots 300\,\mathrm{pF}$ range [6] consumes $1.4\,\mathrm{mA}$ from $5\,\mathrm{V}$ and shows a $\sigma = 63\,\mathrm{aF}$ in $100\,\mathrm{ms}$-measurements, which corresponds to $19.9\,\mathrm{aF}/\sqrt{\mathrm{Hz}}$ input-referred noise. Our interface consumes $1.5\,\mathrm{mA}$ from $3.3\,\mathrm{V}$, which is $71\,\%$ of the power, and has an intrinsic noise below $1.17\,\mathrm{aF}/\sqrt{\mathrm{Hz}}$. Our noise power over $10\,\mathrm{Hz}$ is therefore more than $24\,\mathrm{dB}$ lower than the value reported in [6]. We think our noise power is so much lower because our elaborate offset compensation system allows us to use much more gain in the first stage.

The real state of the art to compare this system to is, however, the field of vortex flowmeters. The system containing our front-end IC can measure down to half the flow compared to previous systems on the market. Since the upper measurement boundary does not change, this means that the dynamic range (turn-down) covered by such instruments has been doubled by this work.

VII. Conclusions

The current-efficient sensor interface IC presented in this paper can measure both the flow speed and the temperature of a medium in a pipe. It has extended the state-of-the-art low-flow boundary for vortex measurements by a factor of two. We have shown how huge offset capacitances (compared to the sensor signal magnitudes) can be compensated even over an extended temperature range. The digital communication interface between sensor IC and remote unit (industry standard is analog) makes the communication more robust, but also causes some digital noise interference that was dealt with on PCB level. The remaining digital interference that couples into the sensor lines does not affect the frequency detection.

References

[1] *Technical Information Proline Prowirl 72F, 72W, 73F, 73W*, Endress+Hauser, accessible on http://www.endress.com/en/products/flow/Product-Vortex-flowmeter-Prowirl-72F, accessed 14-06-03.

[2] J. Meng, L. Zhu, D. Liang, and X. Liang, "Adaptive frequency measurement (AFM) for vortex flowmeter signal," in *Proc. ISIE*, 1992, pp. 832–835.

[3] L. J. Griffiths, "Rapid measurement of digital instantaneous frequency," *IEEE Trans. Acoustics, Speech, Sig. Proc.*, vol. ASSP–23, no. 2, pp. 207–222, Apr. 1975.

[4] M. Rüegg, "Vortex signal analysis based on adaptive prediction filters," Master's thesis, Univ. Appl. Sc. NW Switzerland (FHNW), 2011.

[5] Y. V. Zakharov, G. P. White, and J. Liu, "Low-complexity RLS algorithms using dichotomous coordinate descent iterations," *IEEE Trans. Sig. Proc.*, vol. 56, no. 7, pp. 3150–3161, Jul. 2008.

[6] A. Heidary and G. C. M. Meijer, "Features and design constraints for an optimized SC front-end circuit for capacitive sensors with a wide dynamic range," *IEEE J. Solid-State Circ.*, vol. 43, no. 7, pp. 1609–1616, Jul. 2008.